Theoretical Valence XPS and UV-Visible Absorption Spectra of Four Leuco Dyes Using MO Calculations

Kazuchiyo Takaoka, Sigehiro Maeda, Hidetosi Miura, Kazunaka Endo,*,† and Delano P. Chong*,††

Research Center, Mitsubishi Paper Mills Limited, 46 Wadai, Tsukuba, Ibaraki 300-4247

†Department of Chemistry, Kanazawa University, Kakuma-machi, Kanazawa, Ishikawa 920-11

††Department of Chemistry, University of British Columbia, 2036 Main Mall, Vancouver, B. C. Canada V6T 1Z1

(Received August 13, 1997)

Semiempirical HAM/3 MO program was used to obtain the theoretical valence X-ray photoelectron spectra (XPS) of the two leuco dyes (2′-anilino-6′-diethylamino-3′-methylspiro[isobenzofuran-1(3*H*),9′-[9*H*]xanthene]-3-one (DEAMAF) and 3,3-bis(4-dimethylaminophenyl)-6-dimethylamino-1(3*H*)-isobenzofuranone (CVL)) and UV-visible adsorption spectra of the four leuco dyes (DEAMAF, CVL, 2′-chloro-6′-diethylamino-3′-methylspiro[isobenzofuran-1(3*H*),9′-[9*H*]xanthene]-3-one (DEAMCF), and 3′,6′-bis(diethylamino)-spiro[isobenzofuran-1(3*H*),9′-[9*H*]xanthene]-3-one (Rhodamine B base). The calculated Al $K\alpha$ photoelectron spectra were obtained using Gaussian lineshape functions of an approximate linewidth $0.10E_k$ ($E_k = E'_k - \mathrm{WD}$), where E'_k is the vertical ionization potential (VIP) of each MO and WD is a shift to account for sample work function, polarization energy and other energy effects. On the other hand, the absorption curves were simulated with Gaussian lineshape functions of a constant linewidth of 0.02 eV. The theoretical valence energy levels corresponded well to the spectra of two leuco dyes observed 0—40 eV, while the simulated adsorption spectra were shifted for a good fit with the experimental solution spectra in the range of 250—700 nm.

Leuco dyes are used in heat-sensitive recording systems[1] such as facsimile, wordprocessors, and others. The coloring-to-decoloring reversible reaction of leuco dyes depends upon the acidity and corresponds to open-to-closed forms of the lactone ring. The colored forms are known to be triarylmethine[2] or triphenylmthane dyes. In Fig. 1, we show an example of the reversible reaction with the acidity (The decolored molecule (**1a**) with a lactone ring changes to a colorant (**1b**) (triarylmethine dye) with a quinoid structure by protonation). We think that it would be a very useful step to the design of new materials in heat-sensitive recording system to examine the electronic state of leuco dyes from theoretical and experimental viewpoints.

For triphenylmethane and fluoran dyes, the adsorption spectra were already analyzed to investigate the synthetic design of color dyes[3] by Pariser–Parr–Pople (PPP)[4] method. In the case of 2′-anilino-6′-diethylamino-3′-methylspiro-[isobenzofuran-1(3*H*),9′-[9*H*]xanthene]-3-one (DEAMAF), the structures of decolored and colored types were determined by X-ray diffraction.[5] The structural analyses[6] of coloring and decoloring 2′-chloro-6′-diethylamino-3′-methylspiro[isobenzofuran-1(3*H*),9′-[9*H*]xanthene]-3-one (DEAMCF) were clarified in terms of the ^{13}C NMR and semiempirical Austin Model (AM1)[7] MO methods.

Here, we used the semiempirical Hydrogenic Atoms in Molecules, Version 3 (HAM/3) MO method[8—10] and studied the electronic states of the four leuco dyes (DEAMAF, 3,3-bis(4-dimethylaminophenyl)-6-dimethylamino-1(3*H*)-isobenzofuranone (CVL), DEAMCF, and 3′,6′-bis(diethylamino)-spiro[isobenzofuran-1(3*H*), 9′-[9*H*]xanthene]-3-one (Rhodamine B base)) instead of mentioning HAM/3 at the end. For a good assignment of the valence X-ray photoelectron spectra (XPS) and UV-visible spectra of dyes, we test the semiempirical HAM/3. The HAM/3 method has an advantage over other methods in that the results can be directly compared with experimental data without energy axis correction, because it uses the idea of transition state[11] rather than Koopmans' theorem to predict vertical ionization potentials (VIPs). This method was extended by Chong[12] to interpret many kinds of electron spectroscopy.

Recently the HAM/3 program was applied to the simulation of the photoelectron spectra for carbazole and its five derivatives,[13] the determination of electron affinities for adenine and guanine,[14] and the analysis of XPS for 2-trifluoromethyl-piperazine.[15] In the present paper, we analyzed the valence XPS of DEAMAF and CVL, and the UV-visible absorption spectra of colored and decolored DEAMAF, CVL, DEAMCF, and Rhodamine B dyes by the HAM/3 MO Calculations.

Experimental

1. Materials. We used the commercially available leuco dyes (2′-anilino-6′-diethylamino-3′-methylspiro[isobenzofuran-1(3*H*),9′-[9*H*]xanthene]-3-one (DEAMAF) (Yamamoto Chemicals, Inc.), 3,3-bis(4-dimethylaminophenyl)-6-dimethylamino-1(3*H*)-isobenzofuranone (CVL) (Hodogaya Kagaku Co., Inc.), 2′-chloro-6′-diethylamino-3′-methylspiro[isobenzofuran-1(3*H*),9′-[9*H*]-xanthene]-3-one (DEAMCF) (Nippon Soda Co., Inc.), and 3′,6′-

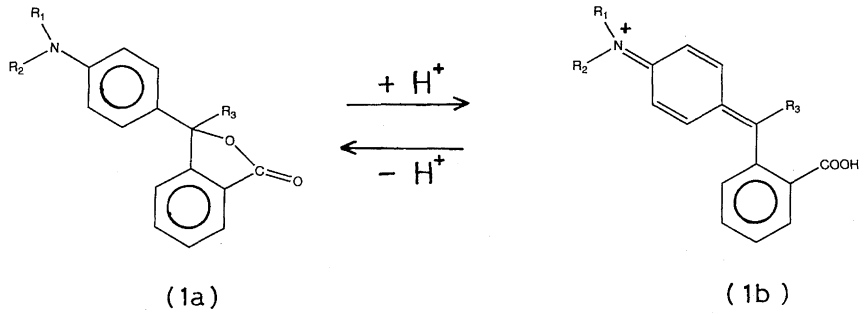

Fig. 1. Reversible reaction of the cleavage of lactone ring for triarylmethine dye by protonation. The structure formula (1a) changes to the colorant (1b) with a quinoid structure by protonation. (R_1, R_2) and R_3 show alkyl and aryl groups, respectively.

bis(diethylamino)-spiro[isobenzofuran-1(3*H*),9′-[9*H*]xanthene]-3-one (Rhodamine B base) (Aldrich Chemical Co., Inc.)).

2. X-Ray Photoelectron Spectra (XPS). The experimental photoelectron spectra of the two leuco dyes, DEAMAF and CVL, were obtained on PHI 5400 MCESCA spectrometer, using monochromatized Al $K\alpha$ radiation (1486.6 eV). The spectrometer was operated at 600 W, 15 kV, and 40 mA. A pass energy of 35.75 eV was employed for high-resolution scans in a valence-band analysis in the range of 50 eV. The angle between the X-ray source and the analyzer was fixed at 45°. The spot size in the measurement was 3×1 mm^2.

The use of dispersion compensation yielded an instrumental resolution of 0.5 eV FWHM (full width at half-maximum) on the Ag3d line. Multiple-scan averaging on the multichannel analyzer was used for the valence-band region due to a very low emission cross section.

For two leuco dyes, we used the pressed thin discs. Gold of 20 Å thickness was deposited on the discs of the dye samples using an ion sputter unit (Hitachi E1030) for the scanning electron microscope.

A low-energy electron flood gun was used in order to avoid any charging effect on the surface of the sample. We used the Au4f core level of the gold decoration film as a calibration reference. The C1s line positions of phenyl rings on the dyes could be fixed at 285.0 eV.

3. UV-Visible Absorption Spectra. In Figs. 2, 3, and 4, we show the three leuco dyes (DEAMAF, CVL, and Rhodamine B base) and their reversible reactions by the acidity to the colorants in structural formula. The decolored DEAMAF (**2a**) in Fig. 2 changes to the colored type (**2b**) with a quinoid structure through the cleavage of a lactone ring by protonation (similar reversible reaction of DEAMCF was omitted). Figures 3 and 4 showed the reversible reaction of CVL and Rhodamine B base to colorants with quinoid resonance structures, respectively.

We obtained the UV-visible absorption spectra of the four leuco dyes (DEAMAF, CVL, DEAMCF, and Rhodamine B base) in decoloring chloroform solution using a Shimadzu UV-3100 spectrometer at room temperature (25 °C). The molar ratio of the dye sample solution was adjusted to 1.5×10^{-5}. For the coloring solution of DEAMAF and DEAMCF, the sample solution contained 1.5×10^{-5} M dye (1 M = 1 mol dm^{-3}) in chloroform including a small amount of H_2SO_4/ethanol (ethanol was used as a stabilizer for chloroform). The molar ratios of the solution were 1/5 and 1/0.008 for the dye/H_2SO_4 and chloroform/ethanol, respectively. In the case of the solution of Rhodamine B (which is the colored form of Rhodamine B base), we adjusted the concentration of the dye as 1.5×10^{-5} M and the molar ratio of dye/H_2SO_4 as 1/10. For coloring solution of CVL, the sample solution contained 6.0×10^{-5} M CVL in chloroform including a small amount of HNO_3/ethanol. The molar ratios of the solution were 1/10 and 1/0.008 for CVL/HNO_3 and chloroform/ethanol, respectively.

Practical Details of MO Calculations. The electronic structures of the dyes (DEAMAF, CVL, DEAMCF, and Rhodamine B base) were calculated by new version of HAM/3 program extended by Chong.[12] For the geometry of the dye molecules, we used the cartesian coordinates optimized with the semiempirical AM1 (version 5) method.[7] For DEAMCF, we used the molecular structure with methyl group instead of Cl atom in the HAM/3 program. In the case of colored dyes, we calculated the electric charge of the dye molecules as a cation.

For the comparison between calculations for molecules in vacuum and experiments on solid or in solution, we must shift each computed energy value E_k' by a quantity σ as $E_k = E_k' - \sigma$, to convert to ionization energy E_k relative to the Fermi level on solid, and to do due to solvent effect and other energy effects. The quantity σ on solid corresponds to WD[16—18] which denotes the sum of the dye work function and other energy effects (polarization energy and so

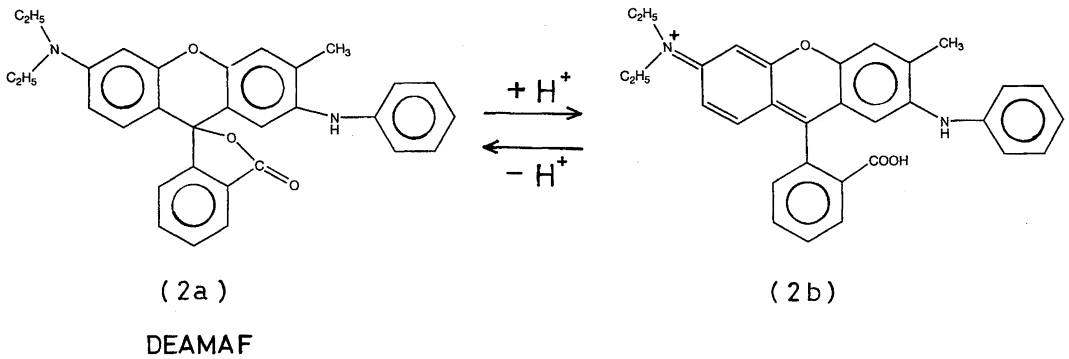

DEAMAF

Fig. 2. Reversible reaction of DEAMAF by protonation (2a and 2b show decolored and colored types, respectively).

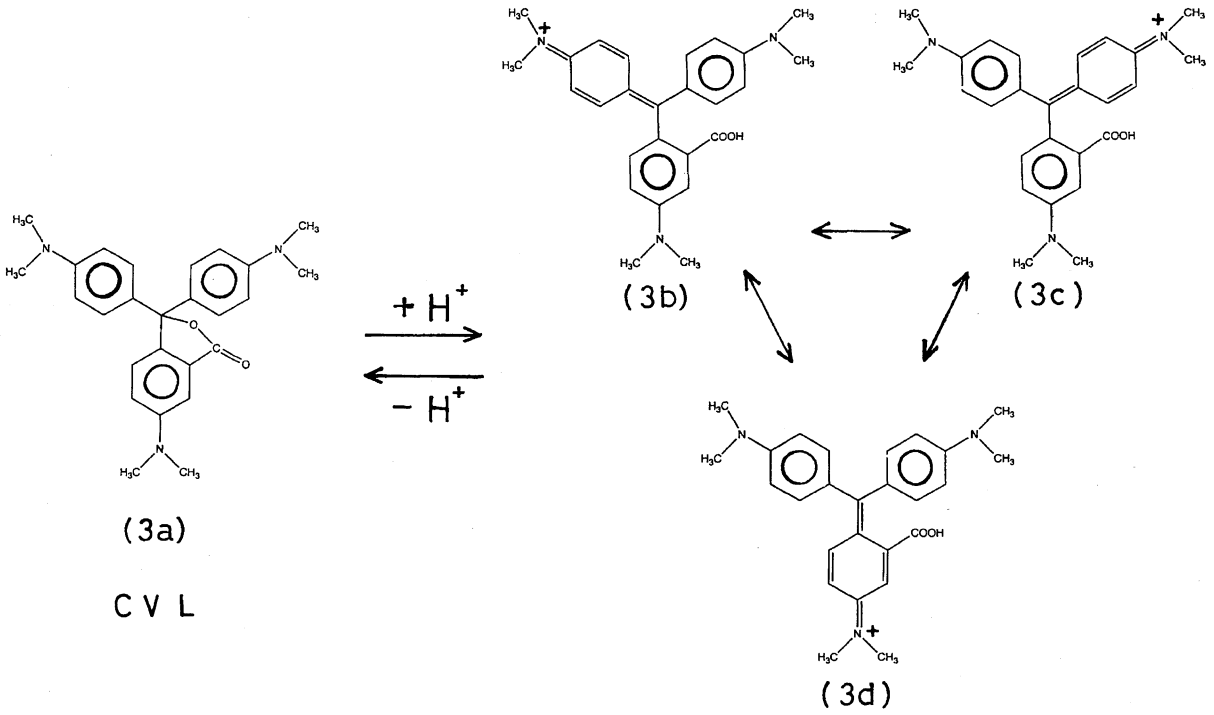

Fig. 3. Reversible reaction of CVL by protonation (3a and 3b show decolored and colored types, respectively).

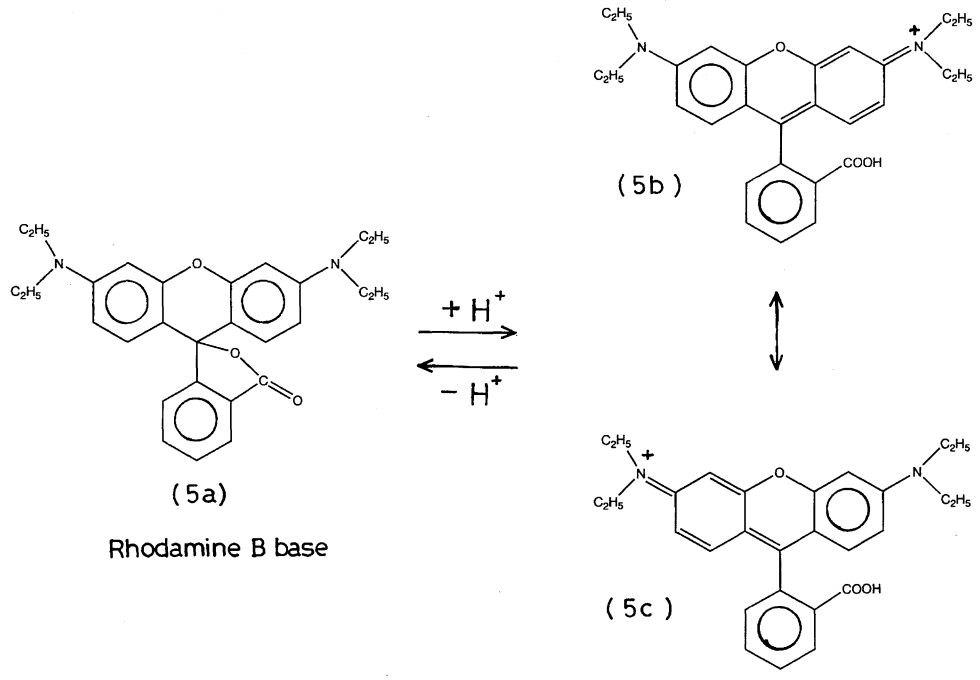

Fig. 4. Reversible reaction of Rhodamine B base by protonation (4a and 4b show decolored and colored types, respectively).

on).

The intensity of the photoelectron was estimated from the relative photoionization cross section for Al $K\alpha$ radiation using Gelius intensity model.[19] For the relative atomic photoionization cross section, we used the theoretical values from Nefedov et al.[20] as the computer output in the HAM/3 program.

The intensity of UV-visible absorption spectra was obtained from the transition probabilities of each transition energy by the configuration interaction method in the HAM/3 program.

The valence XPS and UV-visible absorption spectra of the dyes were simulated by the superposition of a peak centered on the shifted energy values, E_k. Each peak shape is represented by a Gaussian lineshape function:

$$F(x) = A(k)\exp\{-B(k)(x - E_k)^2\} \quad (1)$$

where the intensity, $A(k)$, is estimated from the relative photoion-

ization cross section of Al $K\alpha$ radiation for the valence XPS and the transition probabilities for the UV-visible absorption spectra, respectively. For $B(k)$, we use the linewidth 0.10 E_k for the valence XPS, and a constant linewidth of 0.02 eV for the UV-visible spectra, respectively.

Results and Discussion

(a) Valence XPS of DEAMAF and CVL. In Figs. 5 and 6, the simulated spectra of DEAMAF and CVL with the spectral patterns appear to show fairly good agreement with the observed XPS, although peaks simulated in the range of 20—26 eV are too high to match the observed ones. In the figures, the simulated spectra of DEAMAF in both decolored and colored forms seem to be similar curves. It must, thus, be deduced that we cannot find the difference of the steric forms between decolored and colored dyes, as described in previous work[16] for stereoisomers of polymers. On the other hand, in the case of CVL, there are little differences at around 17 eV and in the range of 7—13 eV between the two simulated decolored and colored types. The results seem to be due to the difference of π-electron conjugated canonical structures between the decolored and colored types: The colored type has a quinoid structure.

For DEAMAF and CVL dyes (in Figs. 5 and 6), the intense peak at around 14 eV corresponds to ionizations from sσ (C2s–C2s, C2s–O2s, C2s–N2s) and pσ (C2s–O2p, C2s–N2p, C2s–C2p)-bonding orbitals. In the figures, we can see that the broader peaks in the range of 17—27 eV are due to the O2s, N2s, and C2s photoionization cross sections which result from sσ (O2s–C2s, N2s–C2s, C2s–C2s) and pσ (O2s–C2p, N2s–C2p)-bonding orbitals. In Tables 1 and 2, we showed the main atomic photoionization cross section, the orbital nature and the functional groups of DEAMAF and CVL, respectively. The WD values were estimated to be 6.0 eV for both dyes. The Fermi level of dyes was estimated to be −6.0 eV from the value obtained as 4.5—6.0 eV of WD for polymers in previous works.[16—18,21,22]

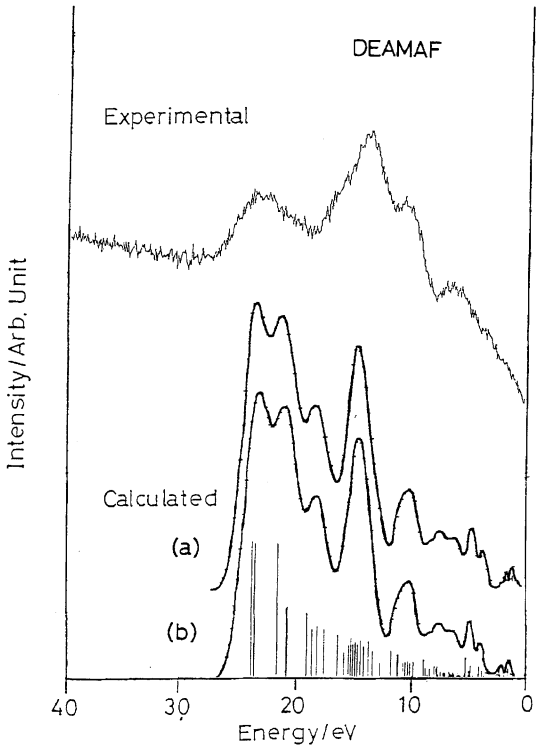

Fig. 5. Valence XPS of DEAMAF with the simulated spectra of the single molecule.(a) simulated decolored form (b) simulated colored form.

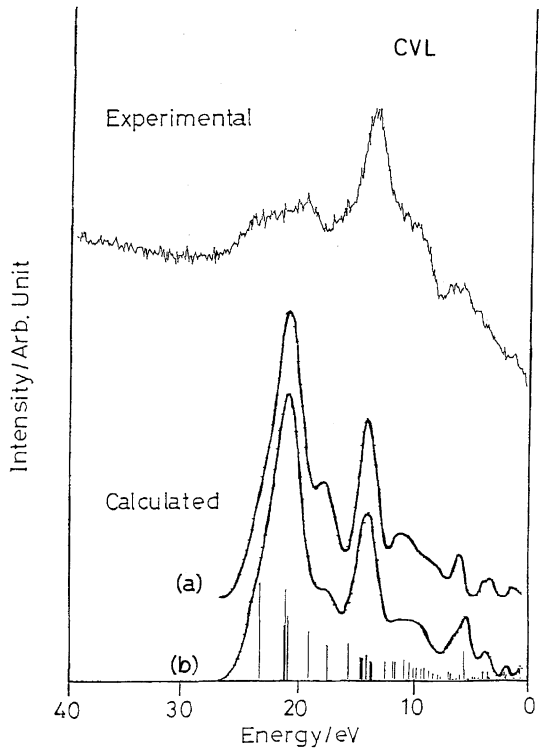

Fig. 6. Valence XPS of CVL with the simulated spectra of the single molecule. (a) simulated decolored form and (b) simulated colored form.

(b) UV-Visible Absorption Spectra of Four Dyes. b-1) DEAMAF. By considering the molecular models of dyes using the MO calculations, we can determine the structure of the dyes in decolored and colored forms. In Fig. 7, we showed optimized molecular structures of DEAMAF determined by an AM1 program. For the decolored form ((**2a**) in Fig. 2), the xanthene moiety was found to be folded at about 180 degrees around the C(spiro)–O(xanthene) axis (in Fig. 7(B)); the lactone moiety is almost perpendicular to the xanthene. The bond length of C(spiro)–O(lactone) at the lactone ring in Fig. 7(A) was calculated to be 1.48 Å, which is longer than the normal C(sp^3)–O bond length (1.43 Å). This means that the cleavage of the lactone ring occurs here. In Fig. 7(C), we showed the optimized molecular structure in the colored form of the cation of DEAMAF ((**2b**) in Fig. 2). In Fig. 8(A) and (B), the bond-order is shown in decolored and colored forms for an optimized molecular structure using the semiempirical AM1 MO method. In the colored form, the diethylaniline ring to the xanthene has a quinoid structure. The optimized decolored and colored structures seem to correspond well to the observed visible spectra in Fig. 8(A)

Table 1. Observed Peaks, VIP, Main AO PICS, Orbital Nature and Functional Group for Valence XPS of DEAMAF (The Gap between Observed and Calculated VIPs) = 6.0 eV

Peaks (eV)	VIP (eV)	Main AO PICS	Orbital nature[b)]	Functional group
	30.2, 30.0, 27.9	O2s(0.8), C2s(0.2)	sσ (O2s–C2s)-B	C–O
24	27.1, 27.0	N2s(0.6), C2s(0.4)	sσ (N2s–C2s)-B	C–N
(20—26)[a)]	25.4—24.4	C2s	sσ (C2s–C2s)-B	C–C
14.0			sσ, pσ (C2s,C2p–C2s,2p)-B	C–C
intensive	23.8—17.4	C2s, C2p, N2s, N2p, O2s, O2p	sσ, pσ (C2s,C2p–N2s,2p)-B	C–N
(12—15)[a)]			sσ, pσ (C2s,C2p–O2s,2p)-B	C–O
11.0	17.3—15.1	C2p, O2p	sσ, pσ (C2s–C2p,O2s,O2p)-B	C–C, C–O
(9.0—12)[a)]	14.9	C2p, N2p	pσ (C2s–N2p)-B	C–N
	8.2—11.3	C2p, N2p, O2p	pσ (C2s,C2p–C2s,2p)-B	C–C, C–O, C–N
	8.1	C2p(0.8), N2p(0.2)	pπ (C2p–N2p)-B	C–N
7.0	7.9, 7.5	C2p, O2p	pπ (C2p–O2p)-B	C=O
(2.0—9.0)[a)]	7.4	O2p	pπ (lone pair)-NB	–O–
	6.2	N2p	pπ (lone pair)-NB	–N–

a) Shows the peak range. b) B and NB means bonding and nonbonding, respectively. (C2s–N2a,2p) means (C2s–N2s) and (C2s–N2p), (C2s,2p–O2p) denotes (C2s–O2p) and (C2p–O2p), and so on.

Table 2. Observed Peaks, VIP, Main AO PICS, Orbital Nature and Functional Group for Valence XPS of CVL (The Gap between Observed and Calculated VIPs) = 6.0 eV

Peaks (eV)	VIP (eV)	Main AO PICS	Orbital nature[b)]	Functional group
	29.7, 27.9	O2s(0.7), C2s(0.3)	sσ (O2s–C2s)-B	C–O
20	27.5, 27.4, 27.3	N2s(0.6), C2s(0.4)	sσ (N2s–C2s)-B	C–N
(17—25)[a)]	25.3, 24.5, 24.2	C2s(0.95),N2s(0,05)	sσ (N2s,C2s–C2s)-B	C–N, C–C
14.0	22.2, 21.6	C2s(0.95), O2s(0.05)	sσ (O2s,C2s–C2s)-B	C–O, C–C
intensive	21.1, 21.0, 20.5	C2s	sσ (C2s–H1s)-B	C–H
(12—15)[a)]	20.9—20.5	C2s, N2s	sσ, pσ (N2p–C2s)-B	N–C–H
	19.1—17.5	C2s, N2s	sσ (N2s–C2s)-B	C–N
10.0	17.3—15.9	C2p(0.7), C2s	pπ, pσ (C2s–C2p)-B	C–C
(8.0—12)[a)]	15.7—14.3	C2p(0.6), C2s, N2p, O2p	pπ, pσ (C2p–C2s,N2p,O2p)-B	C–C, C–N, C=O
	14.0, 13.9	C2p, O2p	pπ, Pσ (C2p–C2p,O2p)-B	C=O, C–C
6.0	13.7—7.9	C2p, N2p, O2p	pπ, pσ (C2p–C2p,N2p,O2p)-B	C–C, C–N, C–O
(2.0—8.0)[a)]	7.8, 7.5	O2p	pπ (lone pair)-NB	–O–
	6.7	N2p	pπ (lone pair)-NB	–N–

a) Shows the peak range. b) B and NB means bonding and nonbonding, respectively. (N2s,C2s–C2s) means (N2s–C2s) and (C2s–C2s) and so on.

and (B), respectively.

In order to simulate the visible spectra, we used the method of configuration interaction for DEAMAF in HAM/3 program. The energies at the high intensities on both decolored and colored forms were selected from the output of the calculation. For a best fit of simulated spectra with the observed ones, we shifted the energy levels with −1.45 and −0.22 eV for the decolored and colored type, respectively.

Figure 9 showed the MO diagram of the transitions for absorption spectra of DEAMAF, to clarify the orbital nature. For the decolored form, the absorption spectrum at around 290 nm results from the excitation between the π-bonding HOMO (π-electrons which conjugated in xanthene ring) and π*-antibonding LUMO (π*-electrons which conjugated in lactone ring involving the phenyl group). In the case of the colored form, the absorption spectrum at around 590 nm corresponds to the transition from π-bonding nearest HOMO which is due to π-electrons in xanthene and aniline rings to the π*-antibonding LUMO of xanthene ring. The MO pictures of the transition for the colored form were added at the right hand of Fig. 9.

b-2) CVL, DEAMCF, and Rhodamine B Base. For the simulation of other dyes (CVL, DEAMCF, and Rhodamine B base), we also used the shifted values of energy levels with −1.45 and −0.22 eV for decolored and colored forms, respectively. In Figs. 10, 11, and 12, the simulated spectra with the canonical structures as obtained from bond-orders by AM1 calculations appear to reflect the observed ones. It can be seen in the structural formula of the colored forms that there is a quinoid structure in the *N,N*-diethylaniline rung of

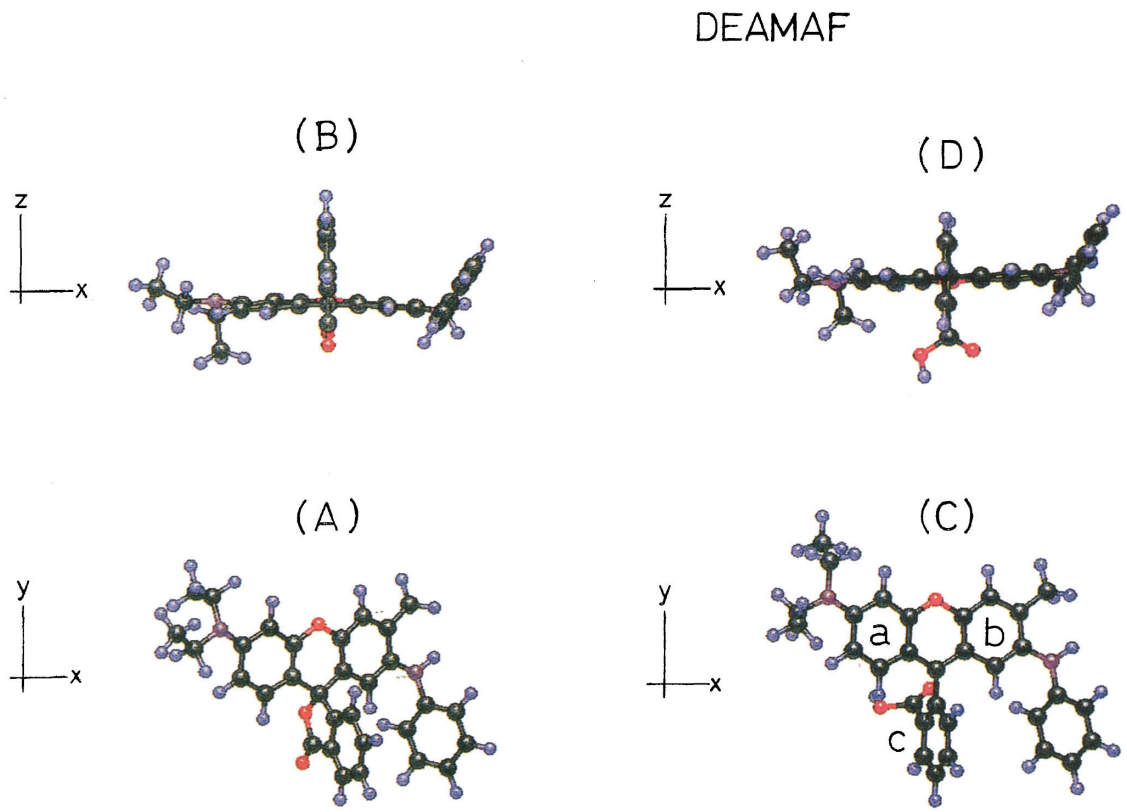

Fig. 7. Optimized molecular models of decolored and colored DEAMAF by AM1 MO calculations. (A) and (B) are the decolored forms of DEAMAF whose lactone ring is closed. (C) and (D) are the colored forms of DEAMAF whose lactone is opened. The xanthene planes of decolored and colored DEAMAF are drawn parallel with *xy*-plane. We observe the molecules from *z*-axis (A, C) and from *y*-axis (B,D).

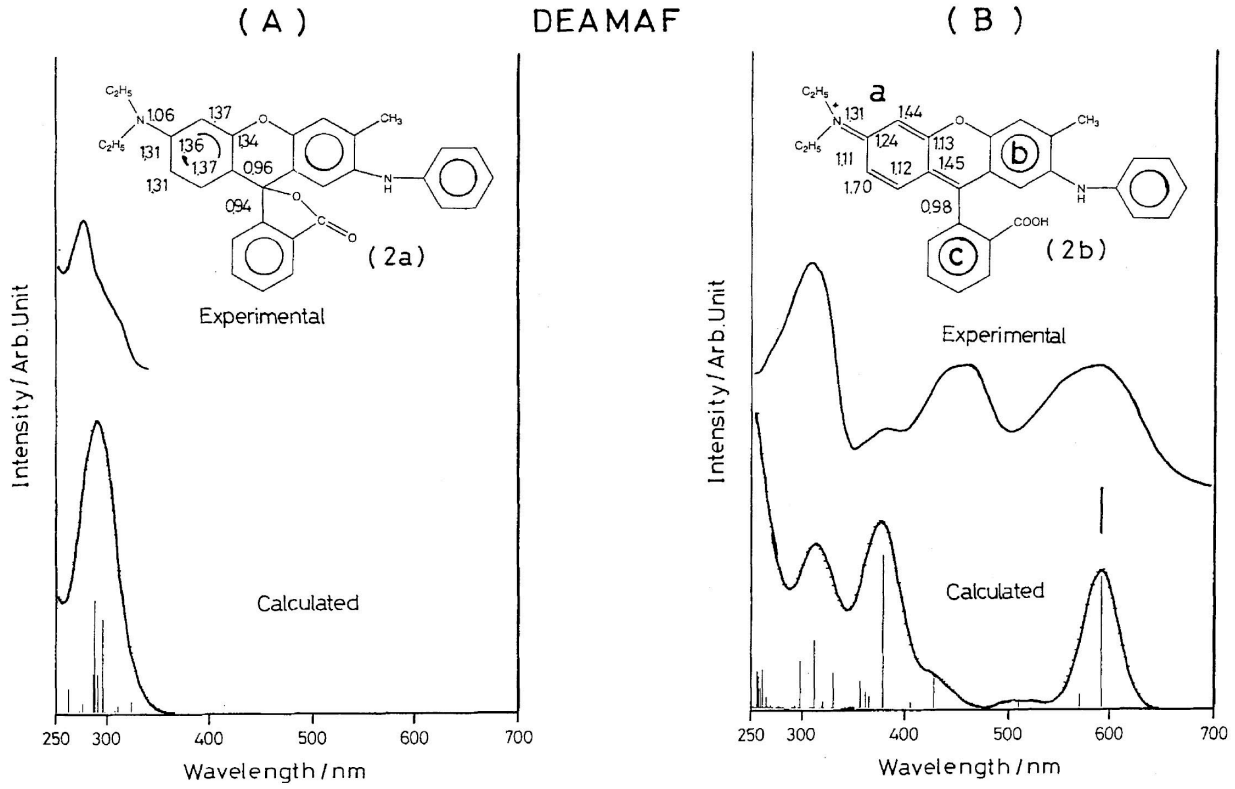

Fig. 8. UV visible absorption spectra of DEAMAF with the simulated spectra of the single molecule. The structural formula was obtained from bond-orders of optimized molecular models by AM1 calculations. (A) spectra in decolored form (B) spectra in colored form.

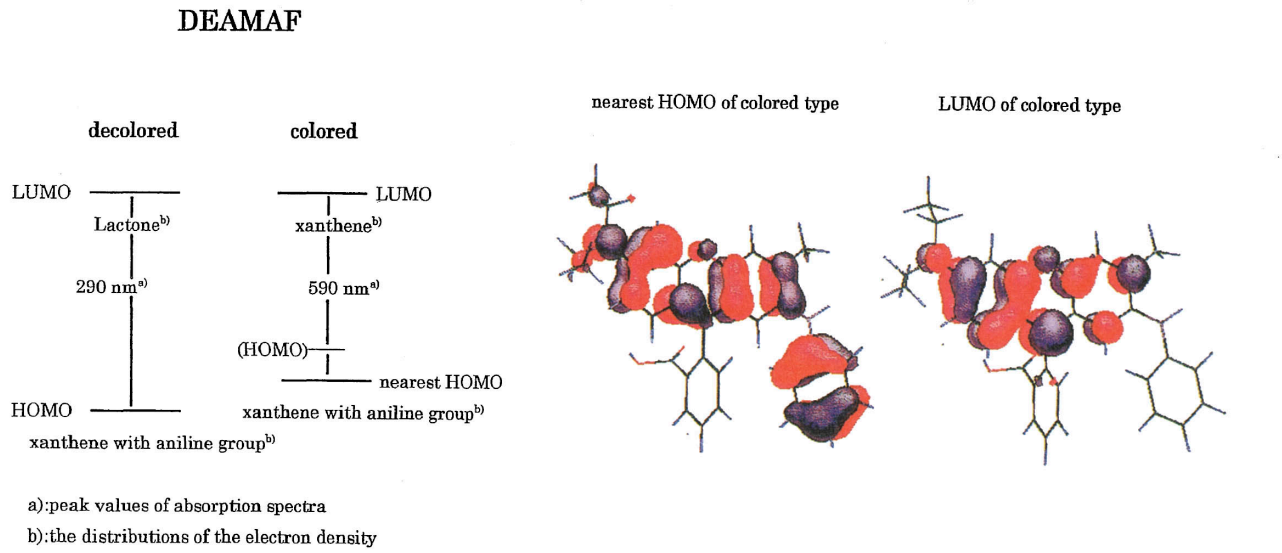

Fig. 9. MO diagram of the transitions for absorption spectra of DEAMAF in decolored and colored types using the method of configuration interaction for single dye molecules in HAM/3 program.

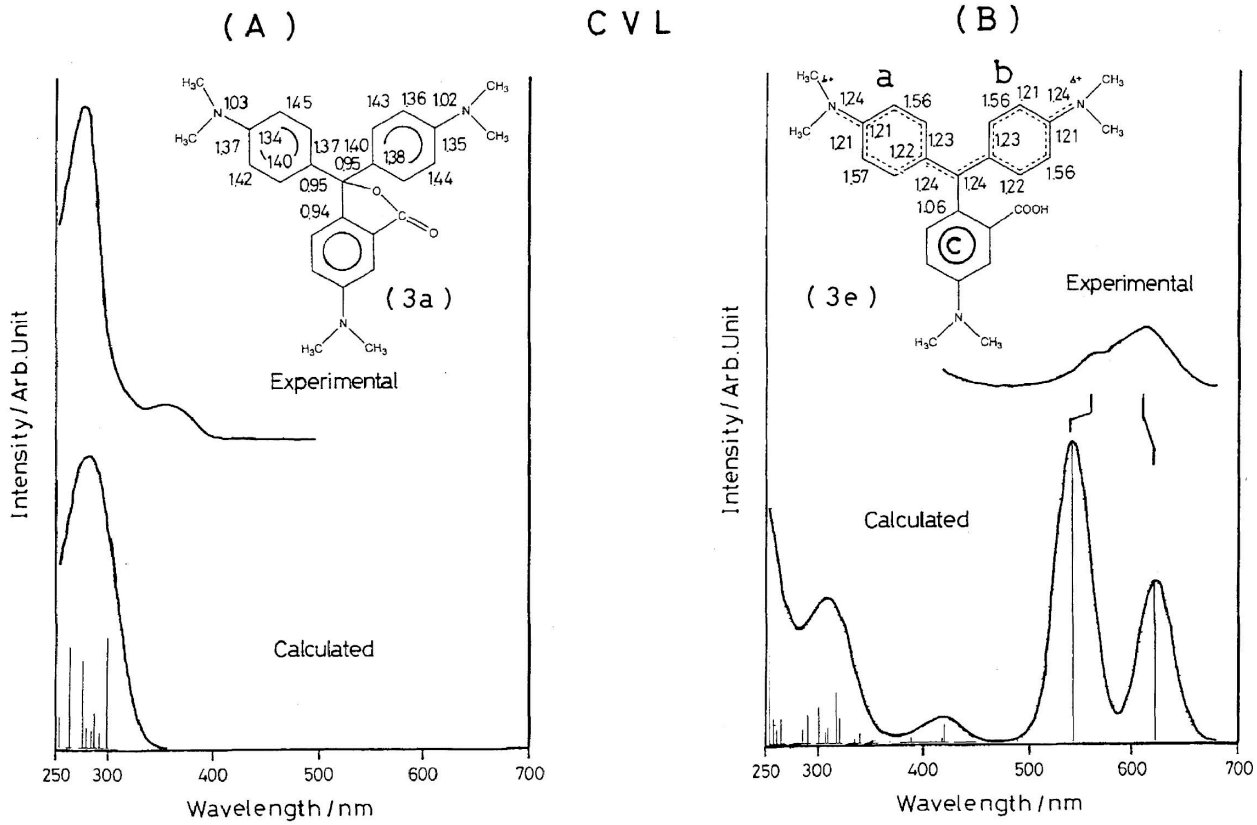

Fig. 10. UV visible absorption spectra of CVL with the simulated spectra of the single molecule. The structural formula was obtained from bond-orders of optimized molecular model by AM1 calculations. (A) spectra in decolored form (B) spectra in colored form.

the xanthene for DEAMCF. For colored CVL, we are able to consider three quinoid resonance structures in Fig. 3, (**3b**), (**3c**), and (**3d**). In the case of Rhodamine B, there are two quinoid resonance structures in the two *N*,*N*-diethylaniline rings in Fig. 4, (4b) and (4c).

In the decolored form of CVL ((**3a**) in Fig. 10), the spectrum at around 280 nm is due to the excitation from π-bonding HOMO (π-electrons of dimethylaminophenyl rings) to the π^*-antibonding LUMO (π-electrons of lactone ring involving phenyl ring). For the colored form, we showed the observed peak (at 620 (X-band) nm) with a shoulder (at 570 (Y-band) nm). The X-band at 620 nm corresponds to the excitation between the π-bonding HOMO (π-electrons of aminophenyl rings ((a) and (b) rings in Fig. 10(B) and π^*-antibonding LUMO (π^*-electrons of three aminophenyl rings ((a), (b), and (c) rings in Fig. 10(B)). The shoulder Y-

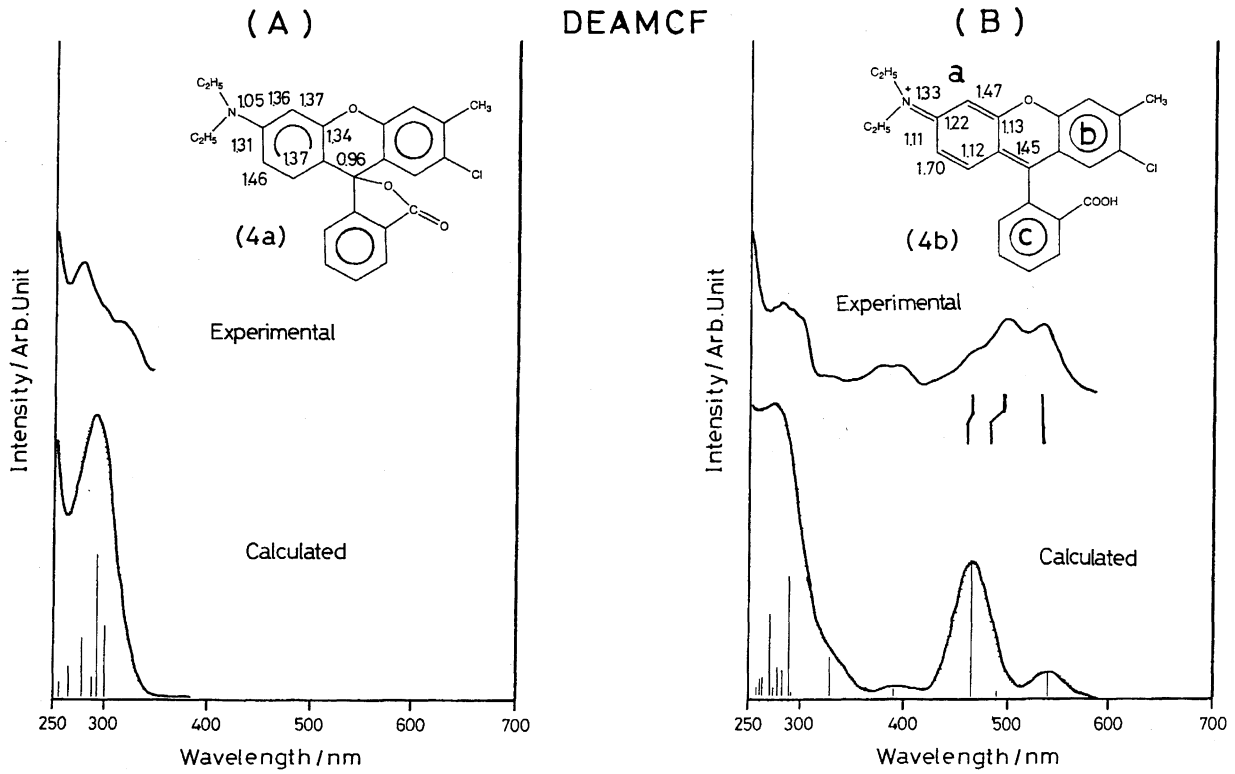

Fig. 11. UV visible absorption spectra of DEAMCF with the simulated spectra of the single molecule. The structural formula was obtained from bond-orders of optimized molecular model by AM1 calculations. (A) spectra in decolored form (B) spectra in colored form.

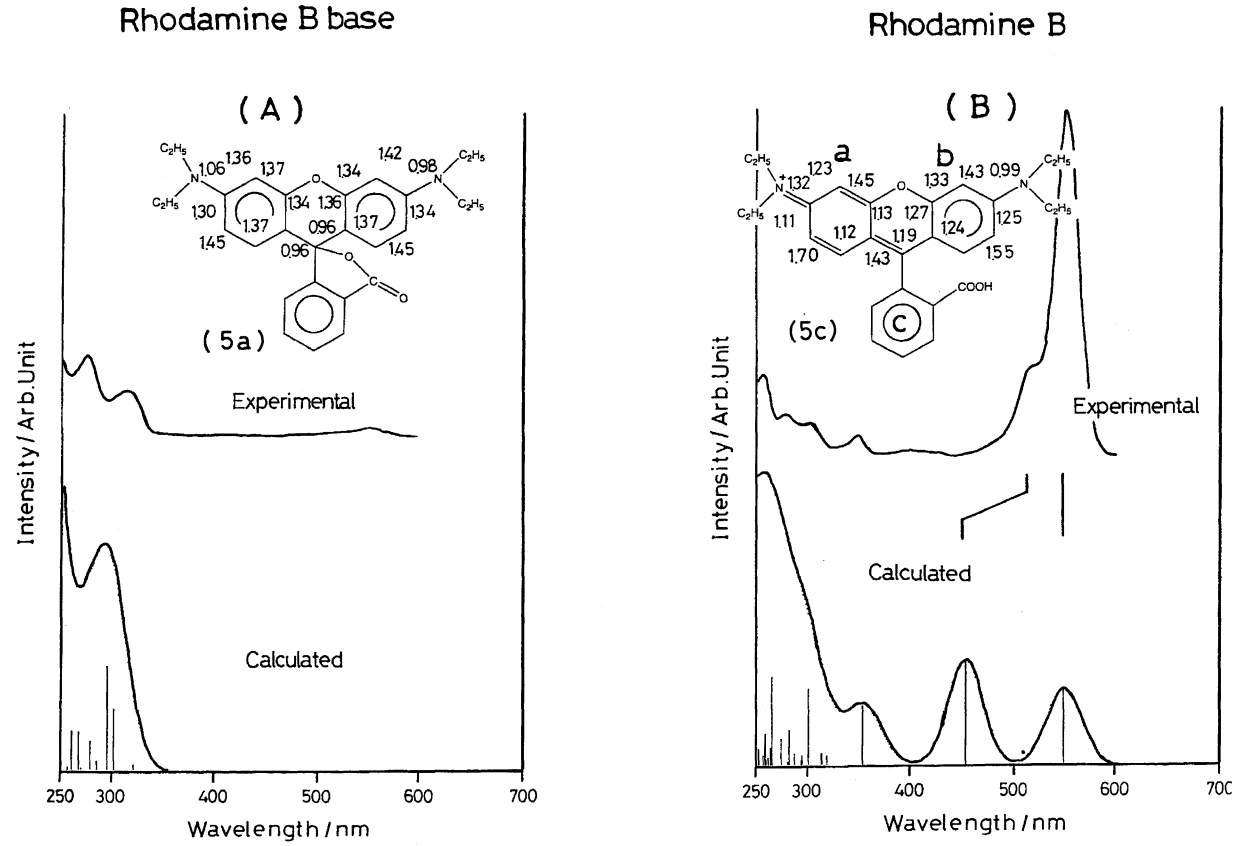

Fig. 12. UV visible absorption spectra of Rhodamine B base and Rhodamine B with the simulated spectra of the single molecule. The structural formula was obtained from bond-orders of optimized molecular model by AM1 calculations. (A) spectra in Rhodamine B base (decolored form) (B) spectra in Rhodamine B (colored form).

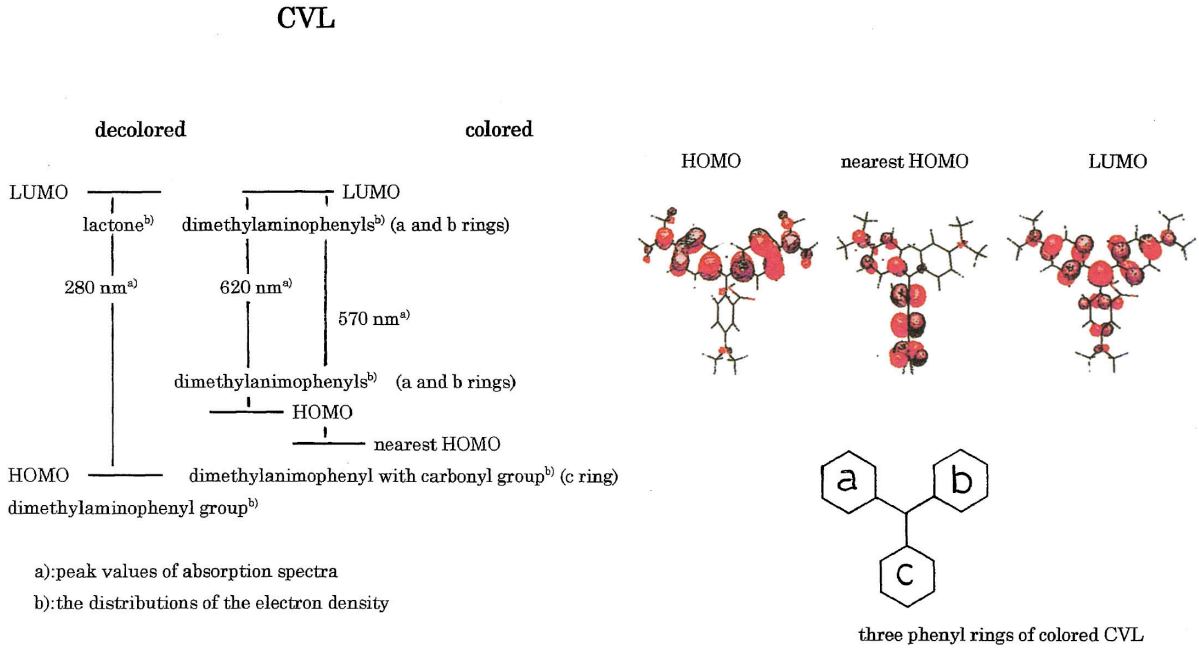

Fig. 13. MO diagram of the transitions for absorption spectra of CVL in decolored and colored types using the method of configuration interaction for single dye molecules in HAM/3 program.

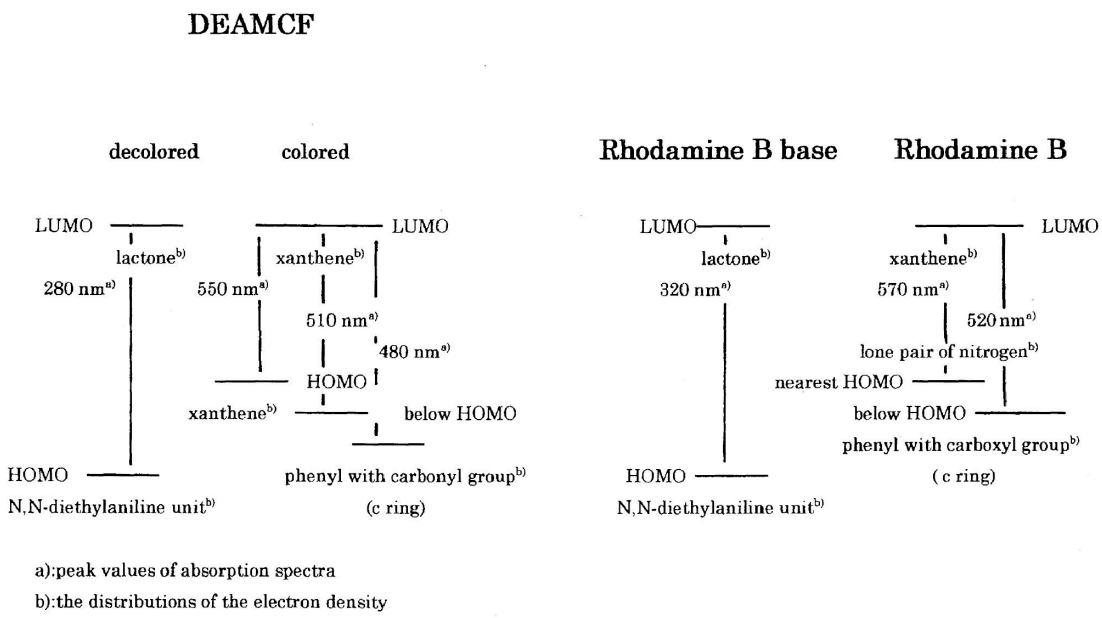

Fig. 14. MO diagram of the transitions for absorption spectra of DEAMCF and Rhodamine B dyes in decolored and colored types using the method of configuration interaction for single dye molecules in HAM/3 program.

band at 570 nm was assumed to result from the transition from the π-bonding nearest HOMO to the LUMO, although the simulated spectrum had a somewhat larger and lower wavelength (at around 540 nm) than the one observed.

In Figs. 11(A) and 12(A), we assumed that the absorption shoulder and peak at 320 nm in decolored form of both DEAMCF and Rhodamine B base, respectively, are due to the transition between π-bonding HOMO (*N*,*N*-diethylaniline unit) and π^*-antibonding LUMO (π^*-electrons of lactone involving phenyl ring). In the case of colored DEAMCF (Fig. 11(B)), the observed absorption peak at 550 nm results from the excitation between π-bonding HOMO (π-electrons of xanthene) and π^*-antibonding LUMO (π^*-electrons of xanthene). The absorption peak and shoulder at 510 and 480 nm seem to correspond to the transition from π-bonding nearest HOMO (π-electrons concentrated in (b) ring of xanthene (Fig. 11(B)) and π-bonding MOs under HOMO (π-electrons of phenyl ring with carboxyl group) to π^*-antibonding LUMO (π^*-electrons of xanthene) for the simulated smaller and larger intensities at around 490 and 470 nm, respectively.

For the colored form of Rhodamine B (Fig. 12(B)), the absorption peak at 570 nm is due to the excitation between π-bonding nearest HOMO (π-type lone-pair electrons on ni-

trogen with aromatic group) and π^*-antibonding LUMO (π^*-electrons of xanthene). The observed absorption shoulder at 520 nm was assumed to correspond to the transition from π-bonding MOs below HOMO (π-electrons of phenyl ring with carboxyl group) to π^*-antibonding LUMO (π^*-electrons of xanthene) for the calculated peak at around 450 nm.

b-3) MO Diagram of Other Dyes. At the left hand Fig. 13, we showed the transitions of decolored and colored forms in MO diagram (the wavelength of the transition denotes observed peaks). In the figure, we show where the distribution of electron density exists for the HOMO and LUMO of each form on CVL molecule. At the right side of Fig. 13, the MO pictures of the transition in the colored form are added. In the MO pictures, the HOMO seems to reflect the resonance quinoid structures, (**3b**) and (**3c**), in Fig. 3, while the nearest HOMO reflects the other structure, (**3d**), in the figure. This corresponds to the results as analyzed for triphenylmethane dyes by PPP calculation.[3)] We can see similar transitions in MO diagrams from experimental and simulated results for absorption spectra of DEAMCF and Rhodamine B base (Fig. 14).

For a comparison between calculations for a single molecules and experiments in solution, we must shift each computed energy levels E'_k by a quantity σ as $E_k = E'_k - \sigma$. When we assume that the quantity σ is due to solvent effect, the polar solvent effects of chloroform to four leuco dyes were estimated as -1.45 and -0.22 eV for decolored and colored cationic molecules, respectively. This means that chloroform causes the blue shift to the leuco dyes, if we can consider $\delta E_{\pi\to\pi^*}$(vacuum) $< \delta E_{\pi\to\pi^*}$ (chloroform) for the difference of the transition energies in vacuum and polar chloroform solution between HOMO and LUMO of four dyes, respectively.

Conclusion

We have analyzed the valence XPS of two dyes (DEAMAF and CVL) and visible absorption spectra of four leuco dyes (DEAMAF, CVL, DEAMCF, and Rhodamine B base) by a semiempirical HAM/3 calculations using the single molecules. The present results suggest several new analytical aspects of the electron spectra:

(1) The HAM/3 method can be used to provide better assignment of the valence XPS of the dyes involving carbon, nitrogen and oxygen. The Fermi level of DEAMAF and CVL was estimated as -6.0 eV from the comparison between calculations for molecules in vacuum and experiments on solid.

(2) We were able to simulate the visible spectra of the four dyes in decolored and colored types using the method of configration interaction for single dye molecules in HAM/3 program.

(a) The simulated spectra of the four dyes with the canonical structures as obtained from bond-orders by AM1 calculations reflected the observed ones.

(b) We clarified the electronic state of the transition for visible absorption spectra of four dyes in decolored and colored types.

(c) Chloroform causes the blue shift to the leuco dyes, if we can consider $\delta E_{\pi\to\pi^*}$(vacuum) $< \delta E_{\pi\to\pi^*}$(chloroform) for the difference of the excitation energies in vacuum and polar chloroform solution between HOMO and LUMO of four leuco dyes, respectively.

References

1) Z. Yoshida and T. Kitao, "Chemistry of Functional Dyes," in "International Symposium in Osaka as the 70th Anniversary of the Founding Proceeding," Kinki Chemical Society, Mita Press, Tokyo (1989).

2) H. Zollinger, "Color Chemistry," Weinheim, New York (1991).

3) M. Matsuoka, K. Ueda, and T. Kitao, *J. Jpn. Soc. Color Mater.*, **55**, 213 (1982).

4) C. Sandorfy, "Electronic Spectra and Quantum Chemistry," Prentice-Hall, Englewood Cliffs, New Jersey (1964); H. Suzuki, "Electronic Spectra and Geometry of Organic Molecules," Academic Press, New York (1967).

5) J. Sueyosi, H. Yoshioka, K. Nakatsu, and Y. Sato, "Annual Meeting of SPSTJ '91," p. 103 (1991).

6) K. Endo, I. Fujita, and N. Kobayasi, *Anal. Sci.*, **7**, 785 (1991).

7) M. J. S. Dewar and E. G. Zoebisch, *Thochem.*, **180**, 1 (1988); M. J. S. Dewar, E. G. Zoebisch, E. F. Healy, and J. J. P. Stewart, *J. Am. Chem. Soc.*, **107**, 3902 (1985).

8) L. Åsbrink, C. Fridh, and E. Lindholm, *Chem. Phys. Lett.*, **52**, 63 (1977); *Quantum Chem. Prog. Exch.*, **12**, 398 (1980).

9) L. Åsbrink, C. Fridh, and E. Lindholm, *Chem. Phys. Lett.*, **52**, 69 (1977).

10) E. Lindholm and L. Åsbrink, "Molecular Orbitals and Their Energies, Studied by Semiempirical HAM Method," Springer-Verlag, Berlin (1985).

11) J. C. Slater, *Adv. Quantum Chem.*, **6**, 1 (1972).

12) D. P. Chong, *Can. J. Chem.*, **63**, 2007 (1985).

13) A. L. Marzinzik, P. Rademacher, and M. Zander, *J. Mol. Struct.*, **375**, 117 (1996).

14) Y. Takahata, *J. Mol. Struct.*, **335**, 229 (1995).

15) L. W. Jenneskenes, J. Mahy, E. M. M. Debrabandervandenberg, I. Vanderhoef, and J. Lugtenburg, *Recl. Trav. Chim. Pays-Bas*, **114**, 97 (1995).

16) K. Endo, C. Inoue, Y. Kaneda, M. Aida, N. Kobayasi, and D. P. Chong, *Bull. Chem. Soc. Jpn.*, **68**, 528 (1995).

17) K. Endo, Y. Kaneda, M. Aida, and D. P. Chong, *J. Phys. Chem. Solids*, **56**, 1131 (1995).

18) K. Endo, Y. Kaneda, H. Okada, D. P. Chong, and P. Duffy, *J. Phys. Chem.*, **100**,19455 (1996).

19) U. Gelius and K. Siegbahn, *Farady Discuss. Chem. Soc.*, **54**, 257 (1972); U. Gelius, *J. Electron Spectrosc. Relat. Phenom.*, **5**, 985 (1974).

20) V. I. Nefedov, N. P. Sergushin, I. M. Band, and M. B. Trzhaskovskaya, *J. Electron Spectrosc. Relat. Phenom.*, **2**, 383 (1973).

21) K. Endo, S. Maeda, and M. Aida, *Polym. J.*, **29**, 171 (1997).

22) K. Endo, S. Maeda, and Y. Kaneda, *Polym. J.*, **29**, 255 (1997).